1965-05

On the structure of pressure systems

Alden, Robert F.; Rosenberger, Glenn C.; Haltiner, G.J.

Monthly Weather Review, Vol. 93, No. 5, pp. 297-305, May 1965.
http://hdl.handle.net/10945/45640

ON THE STRUCTURE OF PRESSURE SYSTEMS

G. J. HALTINER

U.S. Naval Postgraduate School, Monterey, Calif.

and

LT. ROBERT F. ALDEN AND LT. GLENN C. ROSENBERGER

U.S. Navy

ABSTRACT

The three-dimensional distribution of vertical velocity and "isobaric" velocity divergence are numerically evaluated for a number of synoptic situations using Northern Hemisphere data at 1000, 850, 700, 500, and 300 mb. The results indicate that in the typical migratory nondeveloping cyclone only moderate values of divergence exist both in the low and high troposphere with minimum values near 500 mb. On the other hand, a developing cyclone, which deepened markedly at sea level but only slightly in the upper troposphere, displayed much larger values of divergence and vertical velocity, about double; and the level of minimum divergence lowered to 600–700 mb.

In addition, a new pair of positive and negative divergence centers appeared parallel to the east coast of the United States prior to the intensification which took place in the immediate neighborhood.

Similar calculations for a blocking situation gave small values of vertical velocity and divergence in a broad area in the vicinity of the high pressure ridge as contrasted to the normal migratory anticyclonic system.

Finally, computations of thermal advection with the divergent wind showed it to be as much as half of the non-divergent advection at 850 mb., but relatively smaller at upper levels.

1. INTRODUCTION

In the past decade a multitude of models have been developed for the purpose of numerical prediction of the pressure field. A by-product of the experimental and operational use of these models has been the temporal and spatial distribution of certain atmospheric parameters not directly obtainable by conventional observation. At the Naval Postgraduate School and the Fleet Numerical Weather Facility some experiments have been conducted with a five-level prediction model utilizing data at the 1000-, 850-, 700-, 500-, and 300-mb. levels. The procedure involves the solution of the diagnostic vertical velocity equation

$$\nabla^2(\sigma\omega)+\frac{pf\eta}{R}\frac{\partial^2\omega}{\partial p^2}=\nabla^2\left[\frac{g}{f}J(Z,T)\right]-J(T,\eta)-J\left(Z,\frac{g}{f}\nabla^2T\right) \quad (1)$$

as developed by Haltiner, Clarke, and Lawniczak [3]. The vertical velocity is assumed to vanish at an upper boundary of 100 mb.; while at the lower boundary, terrain and friction induce vertical motions which are applied at the height of a smoothed terrain.

The solution of this equation has been carried out twice daily for several years as a part of normal operations. An incidental result has been a greater insight into the structure of pressure systems. Several typical examples will be illustrated including a migratory cyclone during

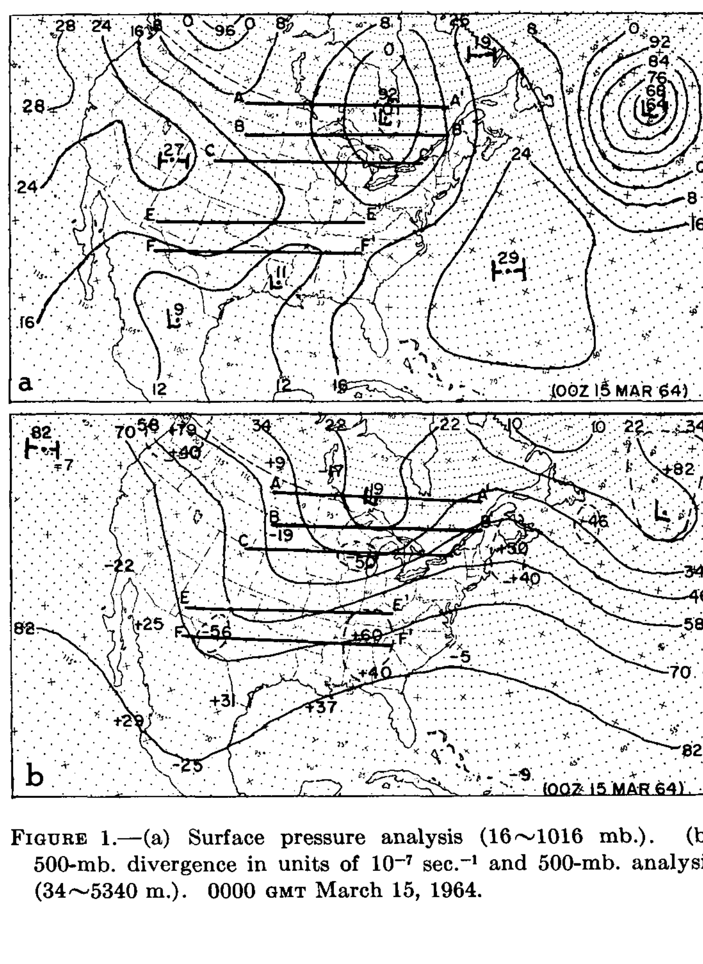

FIGURE 1.—(a) Surface pressure analysis (16∼1016 mb.). (b) 500-mb. divergence in units of 10^{-7} sec.$^{-1}$ and 500-mb. analysis (34∼5340 m.). 0000 GMT March 15, 1964.

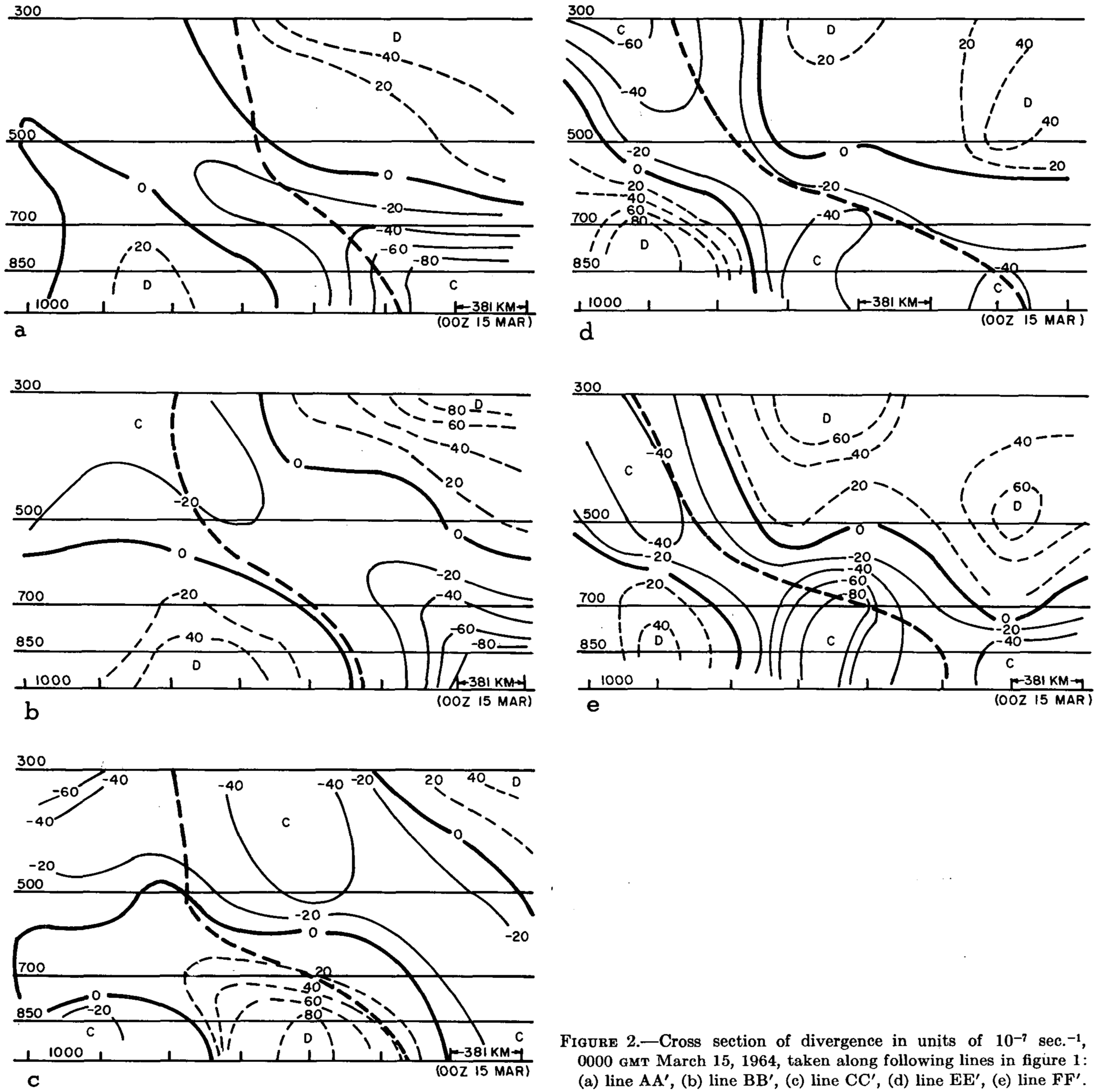

FIGURE 2.—Cross section of divergence in units of 10^{-7} sec.$^{-1}$, 0000 GMT March 15, 1964, taken along following lines in figure 1: (a) line AA′, (b) line BB′, (c) line CC′, (d) line EE′, (e) line FF′.

several stages of development and a blocking High. Emphasis here will be on the distributions of isobaric divergence as obtained from the vertical velocities via the continuity equation

$$\nabla \cdot \mathbf{V} = -\frac{\partial \omega}{\partial p} \tag{2}$$

The data input from five levels provides for considerable vertical resolution, permitting, for example, several levels of nondivergence. All computations were done on a Control Data Corporation 1604 computer over a square grid of 3969 points centered at the North Pole with a grid distance of 381 km. at 60° N. Although the grid covers the Northern Hemisphere, only small areas in the vicinity

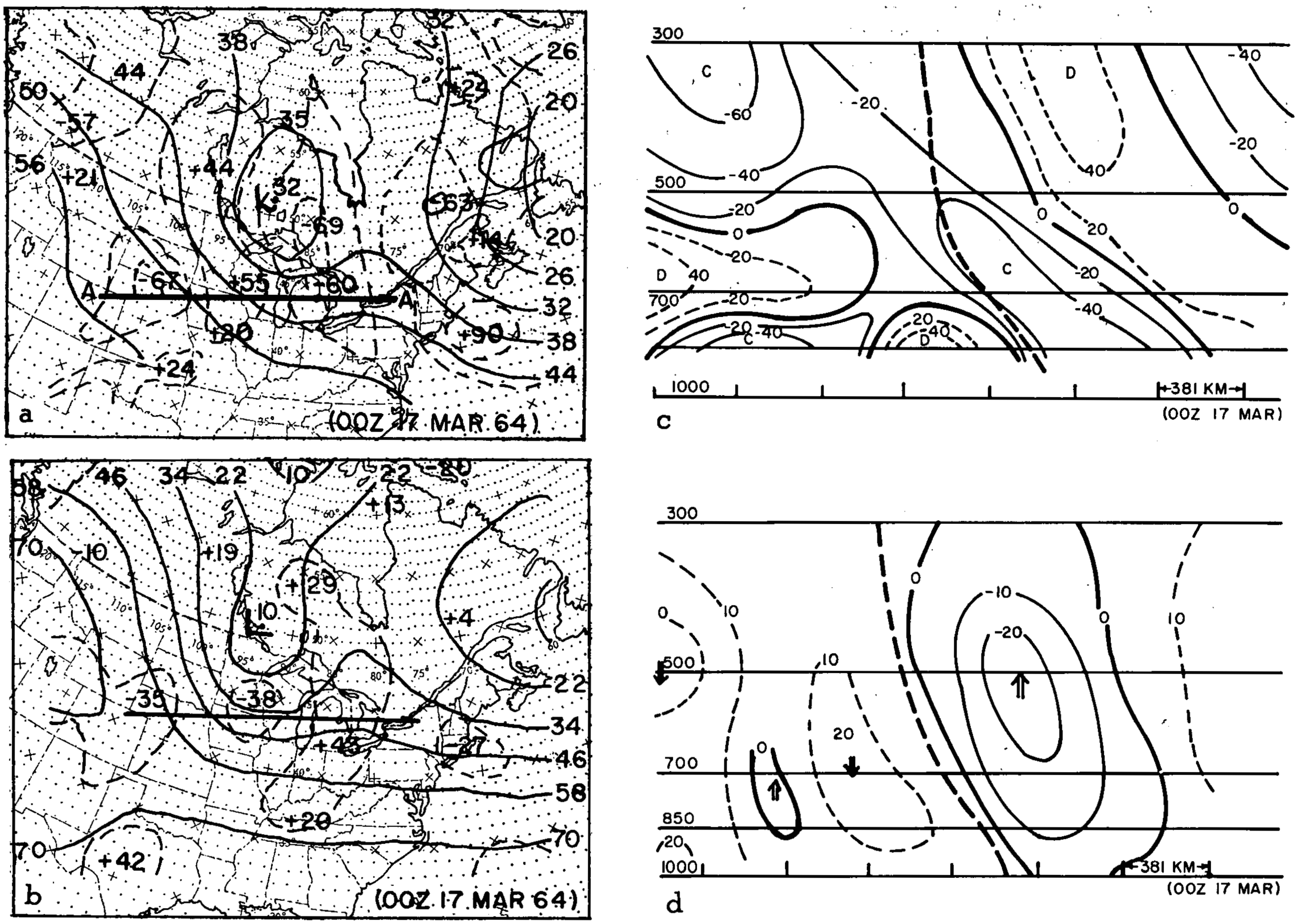

FIGURE 3.—0000 GMT March 17, 1964. (a) 850-mb. divergence and height analysis (50~1500 m.). (b) 500-mb. divergence and height analysis (22~5220 m.). (c) Cross section of divergence taken along line AA′ in 3a. Divergence in units of 10^{-7} sec.$^{-1}$. (d) Cross section of vertical velocity in units of 10^{-4} sec.$^{-1}$ taken along line AA′ in 3a.

of the pressure systems will be exhibited. The few examples shown are considered representative of many other similar cases examined in detail. Moreover, only a small selection of the many charts constructed are actually portrayed; however, it is felt that the pertinent features are included.

2. EXAMPLES

CYCLONE, MARCH 15, 1964

The first case illustrates the variety of patterns of isobaric velocity divergence appearing in different cross sections through a particular trough. Figures 1a and 1b are the surface and 500-mb. analyses for 0000 GMT March 15, 1964, while figure 2 (a–e) shows vertical cross sections depicting velocity divergence (units 10^{-7} sec.$^{-1}$) along the lines AA′, BB′, CC′, EE′, and FF′ of figure 1. The position of the trough line along the vertical is delineated by a heavy dashed line. The patterns are generally similar to the classical concept (see for example, Fleagle [2]) with low-level convergence to the east and near the trough surmounted by high-level divergence, and vice versa to the west. However, there are significant deviations including several levels of nondivergence in some locations and considerable variability along the trough line.

This particular system displayed no significant intensification at any level during the preceding 12 hr. except for a slight increase in circulation at 500 mb., nor did it show any intensification during the next 12 hr. as it moved steadily eastward. This was followed by slight deepening (about 6 mb.) at the surface but not aloft during the following 12 hr. The cross sections appear to suggest that on the average there is a layer of convergence in the vicinity of the trough, though not of large magnitude (see Cressman [1]).

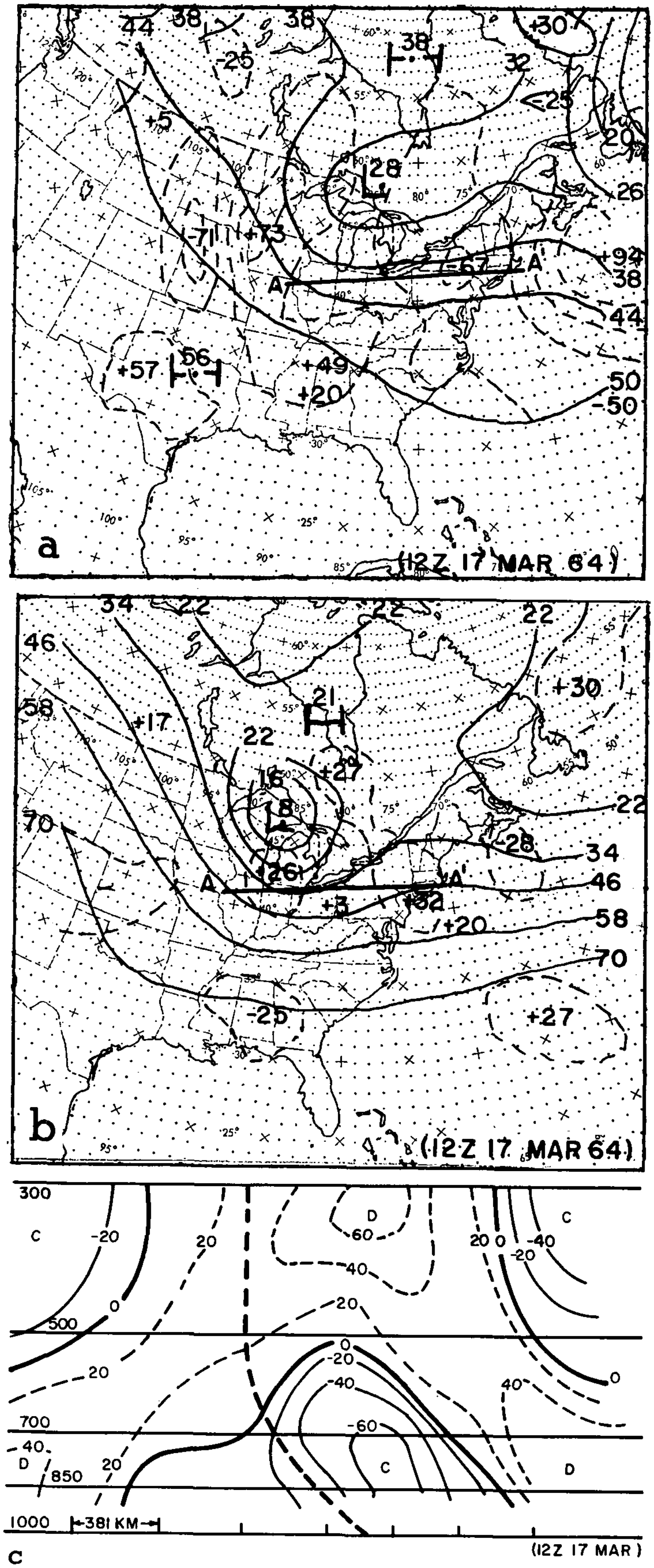

FIGURE 4.—1200 GMT March 17, 1964. (a) 850-mb. divergence and height analysis (50∼1500 m.). (b) 500-mb. divergence and height analysis (22∼5220 m.). (c) Cross section of divergence taken along line AA′ in 4a. Divergence in units of 10^{-7} sec.$^{-1}$.

CYCLONE, MARCH 17–19, 1964

Figures 3a and 3b are the 850- and 500-mb. analyses for 0000 GMT March 17, 1964. The dashed lines represent the isobaric divergence in units of 10^{-7} sec.$^{-1}$. Figures 3c and 3d depict the isobaric divergence and vertical velocity for a vertical cross section along the line AA′ of figure 3a. The magnitudes of these parameters are moderate to small and there was little change of intensity of the cyclone-trough system occurring.

In figure 4 are the 850- and 500-mb. analyses and vertical cross section for 1200 GMT March 17, 1964. The surface Low has filled slightly while the 500-mb. circulation increased considerably though with only slight deepening.

Figures 5a, b, and c are similar charts for 0000 GMT March 18. The system has shown little change in intensity with a steady eastward progression during the past 12 hr. On the other hand, the cross sections of divergence and vertical velocity along the line BB′ (of fig. 5a), as depicted in figures 5d and e, show a line of intensified centers of divergence paralleling the east coast. The level of nondivergence appears near 700 mb. These centers of divergence intensify further on the 1200 GMT March 18 maps shown in figure 6, as well as on the 1000- and 300-mb. maps which are not shown. By this time the sea level cyclone had begun to deepen, about 5 mb. during the past 12 hr.

The 0000 GMT March 19 charts are shown in figure 7. The intensification of the sea level cyclone continued during this period and by 1200 GMT March 19, the central pressure was about 972 mb., reflecting a deepening of over 25 mb. during the past 24 hr. Though the cross sections show strongly developed divergence, the centers of maximum intensity which are southeast of the cross section line, are even larger, as may be observed on the 850- and 500-mb. charts.

The 1200 GMT March 19 charts in figure 8 again show strongly developed centers of divergence and vertical velocity. During the preceding 12 hr. the 500-mb. center deepened about 60 m., a comparatively modest development compared to the marked deepening of the sea level system. The data suggest that the sea level deepening is accompanied by an overall increase in the magnitude of the centers of convergence, divergence, and vertical velocity as well as a lowering of the mean level of nondivergence ordinarily found in the vicinity of 500 mb. The former concept appears to be implied in Sutcliffe's [4] development equation.

BLOCKING SITUATION, FEBRUARY 13, 1964

Figures 9a, b, and c show the distribution of isobaric divergence at the 850- 500- and 300-mb. levels for a "blocking" situation. Note the relatively small magnitudes, particularly aloft, in the vicinity of the ridge. Figures 9d and e display velocity divergence and vertical velocity ω in cross section form along the line shown in figure 9a. Note again the relatively small vertical ve-

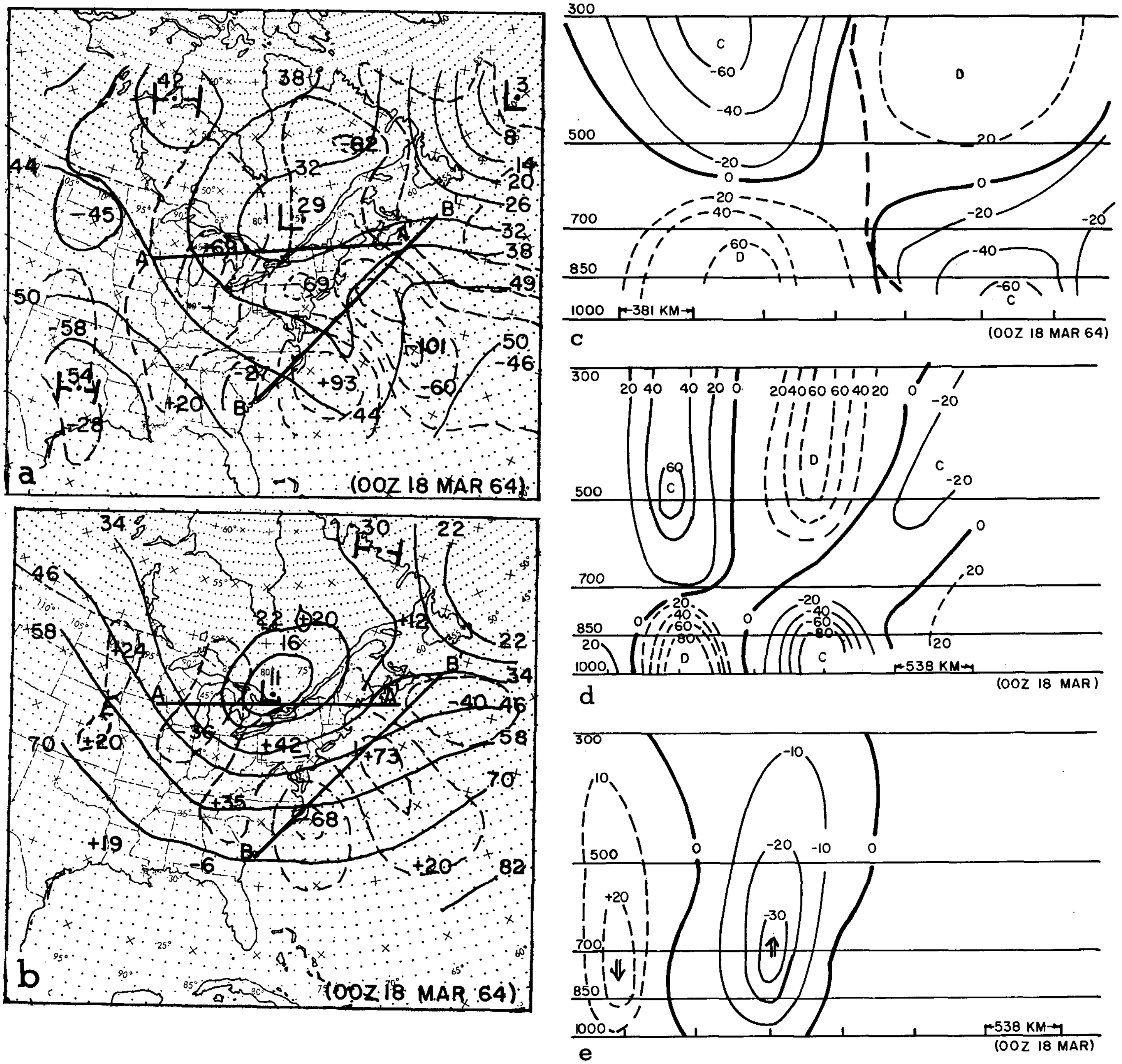

FIGURE 5.—0000 GMT March 18, 1964. (a) 850-mb. divergence and height analysis (50∼1500 m.). (b) 500-mb. divergence and height analysis (22∼5220 m.). (c) Cross section of divergence taken along line AA′ in 5a. (d) Cross section of divergence taken along line BB′ in 5a. Divergence in units of 10^{-7} sec.$^{-1}$. (e) Cross section of vertical velocity in units of 10^{-4} sec.$^{-1}$ taken along line BB′ in 5a.

locities and corresponding isobaric divergence in a fairly broad band extending on either side of the ridge (denoted by a dotted line). The various diagrams clearly indicate the stagnant nature of the blocking situation.

3. THERMAL ADVECTION

Integral relations have demonstrated the need for including the thermal advection with the divergent part of

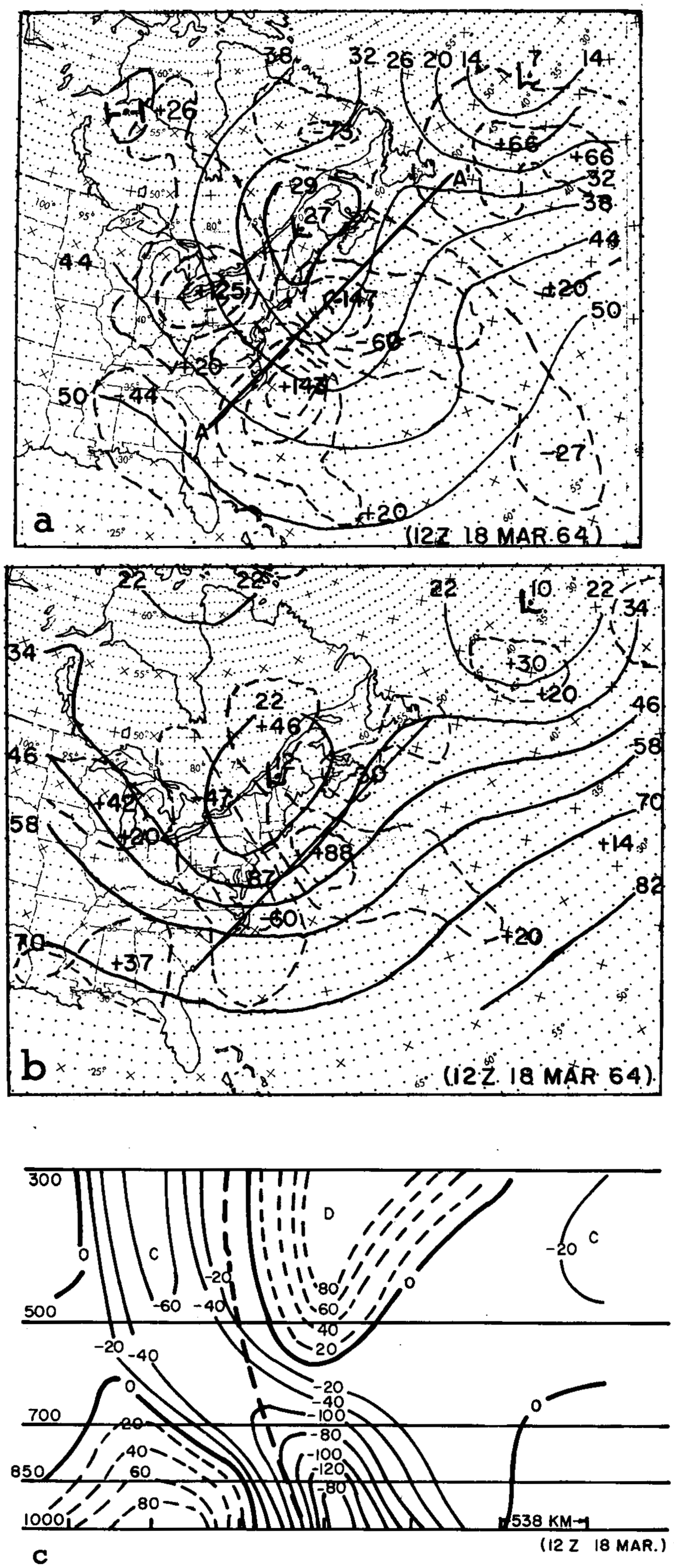

FIGURE 6.—1200 GMT March 18, 1964. (a) 850-mb. divergence and height analysis (50∼1500 m.). (b) 500-mb. divergence and height analysis (22∼5220 m.). (c) Cross section of divergence taken along line AA′ in 6a. Divergence in units of 10^{-7} sec.$^{-1}$.

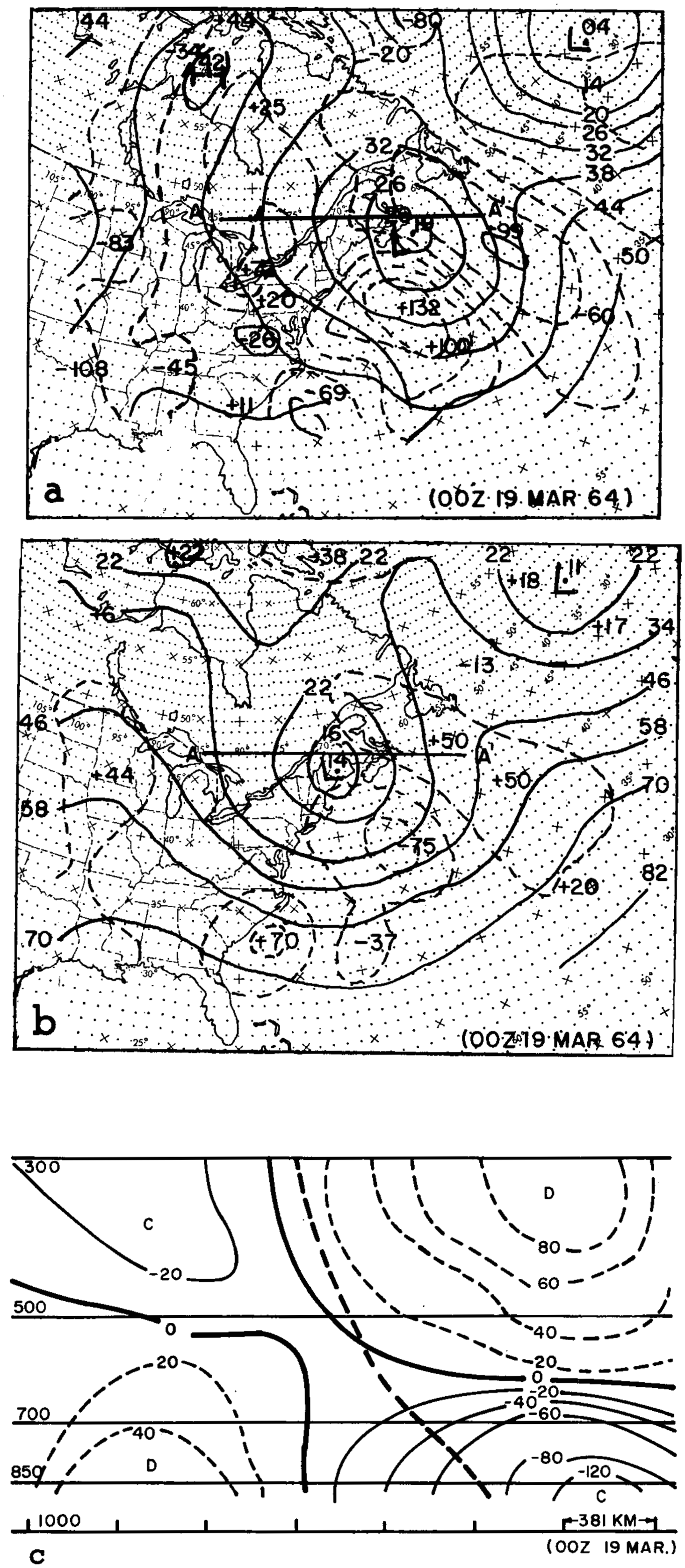

FIGURE 7.—0000 GMT March 19, 1964. (a) 850-mb. divergence and height analysis (50∼1500 m.). (b) 500-mb. divergence and height analysis (22∼5220 m.). (c) Cross section of divergence taken along line AA′ in 7a. Divergence in units of 10^{-7} sec.$^{-1}$.

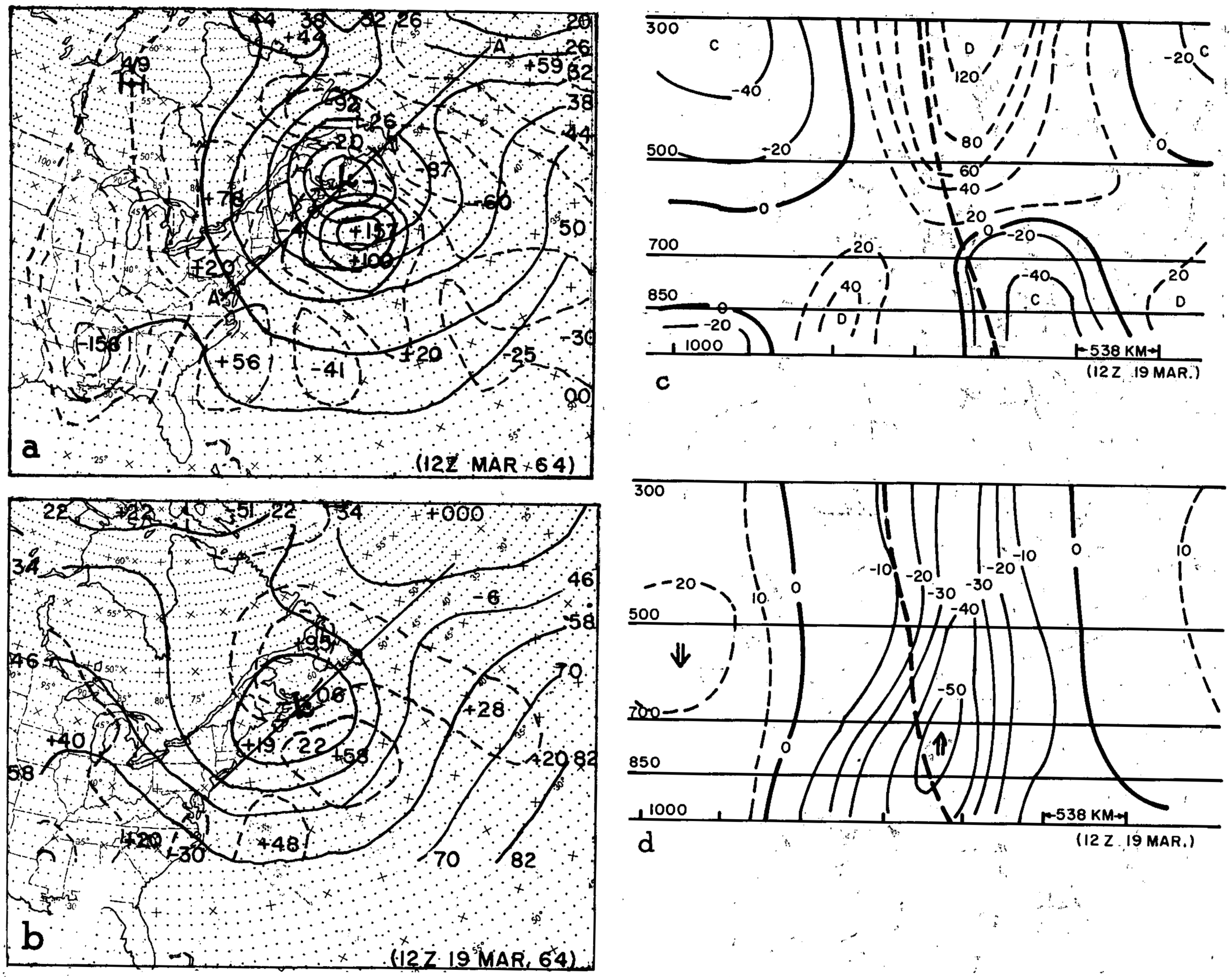

Figure 8.—1200 GMT March 19, 1964. (a) 850-mb. divergence and height analysis (50∼1500 m.). (b) 500-mb. divergence and height analysis (22∼5220 m.). (c) Cross section of divergence taken along line AA′ in 8a. Divergence in units of 10^{-7} sec.$^{-1}$. (d) Cross section of vertical velocity in units of 10^{-4} sec.$^{-1}$ taken along line AA′ in 8a.

the wind if a variable static stability parameter is permitted. Having computed the velocity divergence, only a simple Poisson relaxation is necessary to obtain the velocity potential χ for the divergent wind component $\mathbf{V}_\chi$, namely

$$\nabla^2\chi=\nabla\cdot\mathbf{V}=-\frac{\partial\omega}{\partial p}$$

$$\mathbf{V}_\chi=\nabla\chi$$

This wind was used to compute the thermal advection $-\mathbf{V}_\chi\cdot\nabla T$, for purposes of comparison with advection with the nondivergent wind, $-\mathbf{V}_\psi\cdot\nabla T$, where $\mathbf{V}_\psi=\mathbf{k}\times\nabla\psi$, the stream function ψ being obtained by solution of the balance equation.

An example of this computation is shown in figure 10. Comparison of the centers of maximum magnitude indicates that at 850 mb. the advection with the divergent wind may be easily half the nondivergent advection in some areas and certainly should not be omitted. Thermal advection with the divergent wind was somewhat smaller at 500 mb. in this case.

Obviously, thermal advection with only the nondivergent (or rotational) wind may have significant errors with respect to temperature changes. It is interesting to note nevertheless that a comparison of the prediction

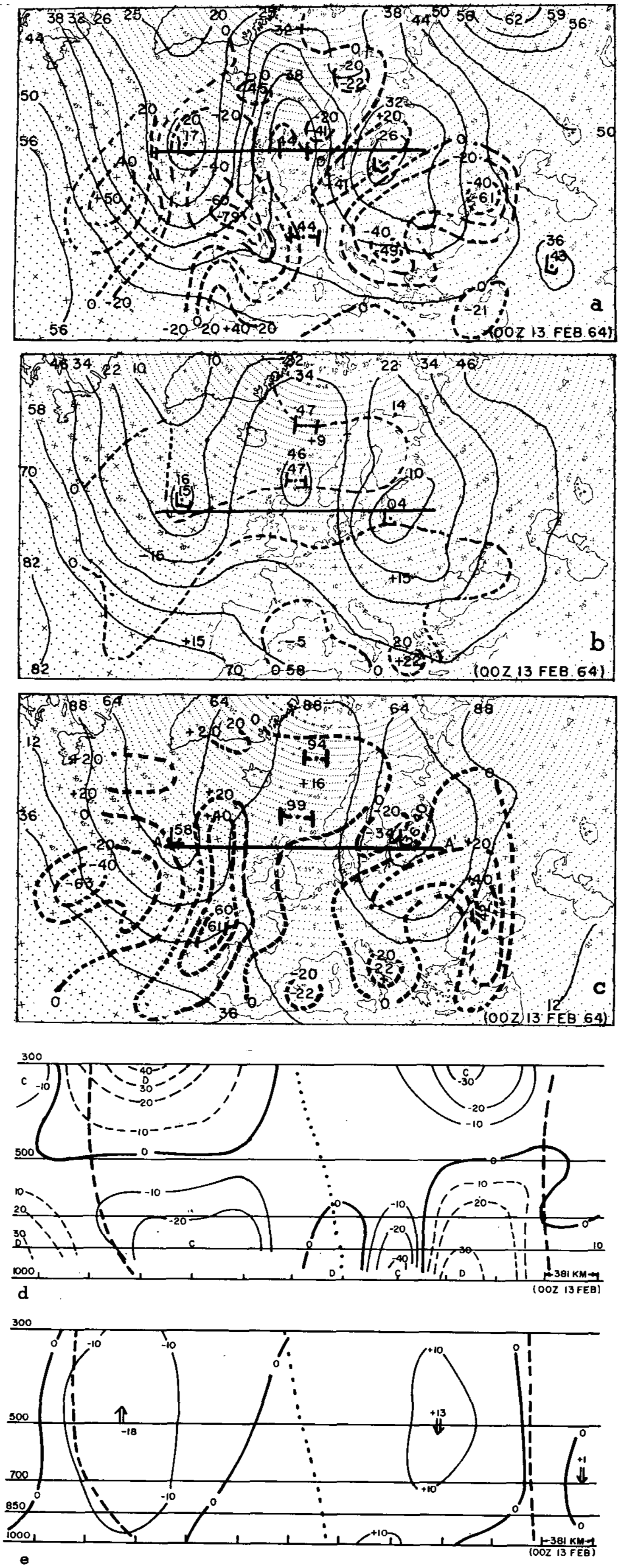

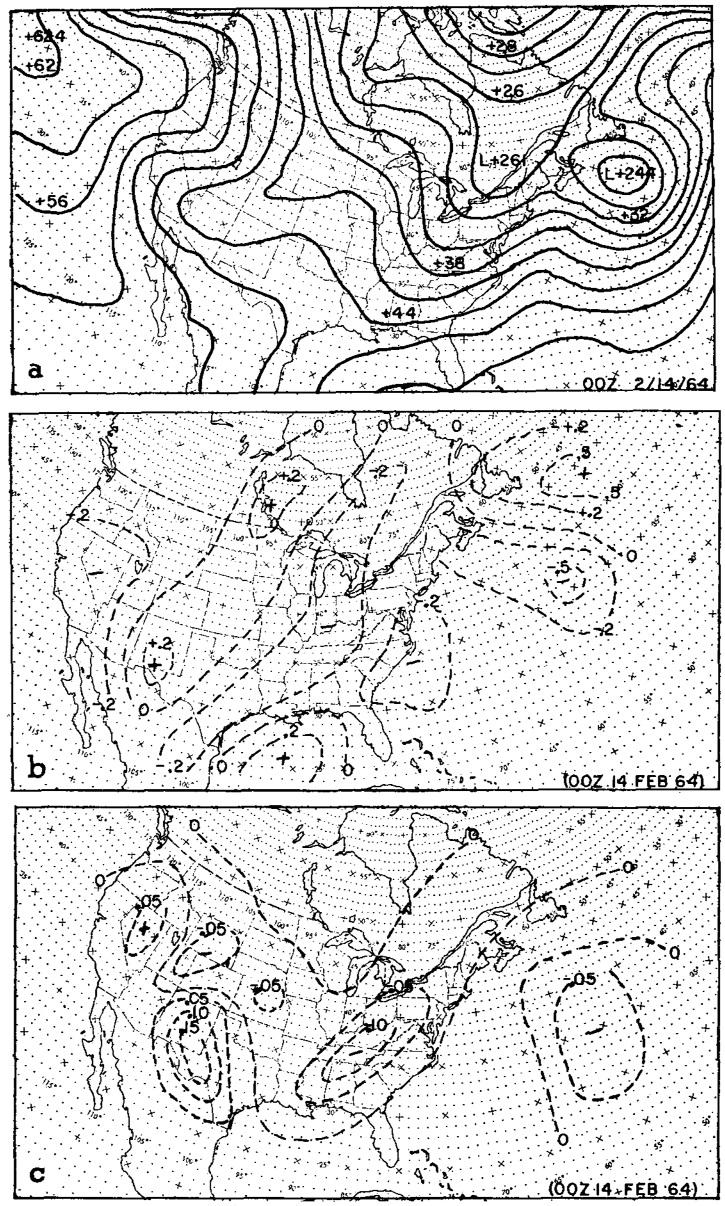

FIGURE 10.—0000 GMT February 14, 1964. (a) 850-mb. height analysis (50∼1500 m.). (b) 850-mb. thermal advection with the nondivergent wind in ° C. hr.$^{-1}$. (c) 850-mb. thermal advection with the divergent wind in ° C. hr.$^{-1}$.

←

FIGURE 9.—0000 GMT February 13, 1964. (a) 850-mb. divergence and height analysis (50∼1500 m.). (b) 500-mb. divergence and height analysis (22∼5220 m.). (c) 300-mb. divergence and height analysis (12∼9120 m.). (d) Cross section of divergence taken along line AA′ in 9c. Divergence in units of 10^{-7} sec.$^{-1}$. (e) Cross section of vertical velocity in units of 10^{-4} sec.$^{-1}$ taken along line AA′ in 9c.

errors of three different five-level baroclinic models, one of which included the divergent (or irrotational) wind component, showed no significant differences. However, since the sample size was very small, the test may not be considered conclusive.

REFERENCES

1. G. P. Cressman, "A Diagnostic Study of Mid-Tropospheric Development," *Monthly Weather Review*, vol. 89, No. 3, Mar. 1961, pp. 74–82.
2. R. F. Fleagle, "Quantitative Analysis of Factors Influencing Pressure Change," *Journal of Meteorology*, vol. 5, No. 6, Dec. 1948, pp. 281–292.
3. G. J. Haltiner, L. C. Clarke, and G. E. Lawniczak, Jr., "Computation of the Large Scale Vertical Velocity," *Journal of Applied Meteorology*, vol. 2, No. 2, Apr. 1963, pp. 242–259.
4. R. C. Sutcliffe, "A Contribution to the Problem of Development," *Quarterly Journal of the Royal Meteorological Society*, vol. 73, Nos. 317–318, July/Oct. 1947, pp. 370–383.

[Received October 21, 1964; revised December 21, 1964]